PROTEINS: Structure, Function, and Genetics 27:110–117 (1997)

Large Differences Are Observed Between the Crystal and Solution Quaternary Structures of Allosteric Aspartate Transcarbamylase in the R State

Dmitri I. Svergun,[1,2]* Claudio Barberato,[1] Michel H. J. Koch,[1] Luc Fetler,[3] and Patrice Vachette[3]
[1]*European Molecular Biology Laboratory, Hamburg Outstation, Hamburg, Germany;* [2]*Institute of Crystallography, Russian Academy of Sciences, Moscow, Russia;* [3]*Laboratoire d'Utilisation du Rayonnement Electromagnetique (CNRS, CEA, MENESR), Universite Paris-Sud, Orsay, France*

ABSTRACT **Solution scattering curves evaluated from the crystal structures of the T and R states of the allosteric enzyme aspartate transcarbamylase from *Escherichia coli* were compared with the experimental x-ray scattering patterns. Whereas the scattering from the crystal structure of the T state agrees with the experiment, large deviations reflecting a significant difference between the quaternary structures in the crystal and in solution are observed for the R state. The experimental curve of the R state was fitted by rigid body movements of the subunits in the crystal R structure which displace the latter further away from the T structure along the reaction coordinates of the T→R transition observed in the crystals. Taking the crystal R structure as a reference, it was found that in solution the distance between the catalytic trimers along the threefold axis is 0.34 nm larger and the trimers are rotated by 11° in opposite directions around the same axis; each of the three regulatory dimers is rotated by 9° around the corresponding twofold axis and displaced by 0.14 nm away from the molecular center along this axis. Proteins 27:110–117**

Key words: small-angle scattering; x-rays; allosteric enzymes; crystal structure; rigid body modeling

INTRODUCTION

Aspartate transcarbamylase (ATCase) from *Escherichia coli* (E.C. 2.1.3.2), one of the most thoroughly studied enzymes has become a classic textbook illustration of allostery.[1] It catalyzes the carbamylation of the L-aspartate amino group by carbamyl phosphate, the first step of the pyrimidine pathway,[2] and its activity shows positive cooperativity for aspartate as well as modulation by nucleotide effectors.[3] Its six catalytic (c) chains c_1—c_6 grouped in two trimers and six regulatory (r) chains r_1—r_6 grouped in three dimers form a 306-kDa assembly with quasi-D_3 symmetry.[4–6] The homotropic cooperative properties of ATCase are broadly compatible with the classical MWC theory of allostery,[7] which is based on a reversible transition between a low-affinity T (tense) and a high-affinity R (relaxed) state. The conformational change associated with the T→R transition was first detected by sedimentation velocity experiments.[8,9] The crystal structures of the two states of ATCase were determined by Lipscomb and coworkers,[6,10–12] and the T→R transition was described essentially in terms of rigid body movements of the c and r subunits. The most prominent movements are the increase in distance between the catalytic trimers by 1.1 nm and their rotation by 6° in opposite directions around the threefold axis, together with the rotation of each of the three r dimers by 15° around the corresponding twofold axes (Fig. 1A,B). These movements are accompanied by the closure of the cleft between the domains in each c chain and by changes in the tertiary structure, such as the reorganization and relocation of the 240s loop forming the contacts between the c trimers.[11]

Small-angle x-ray scattering, which provides information on the global conformation of macromolecules in solution, has proved to be of particular value for the study of the conformational changes associated with the biological properties of oligomeric assemblies. In the case of ATCase, the elongation along its threefold axis upon the T→R transition was predicted from the larger c axis in the R-state crystals than in the T-state crystals,[13] as well as by solution scattering.[14] Small-angle scattering profiles of ATCase calculated from the crystal structures showed changes between T and R similar to those observed experimentally, but with systematic deviations which were attributed to the unaccounted solvent contribution in the theoretical profiles.[15] In

The work was performed at the European Molecular Biology Laboratory, Hamburg Outstation, Hamburg, Germany and the Laboratoire d'Utilization du Rayonnement Electromagnetique, Orsay, France.
Claudio Barberato's present address is Laboratorio Nacional de Luz Sincrotion, C.P. 6192, 13081–970 Campinas, SP, Brasil.
*Correspondence to: Dr. D. Svergun, EMBL c/o DESY, Notkestraße 85, Hamburg, D-22603 Germany. E-mail: Svergun@EMBL-Hamburg, DE.
Received 20 May 1996; accepted 18 July 1996.

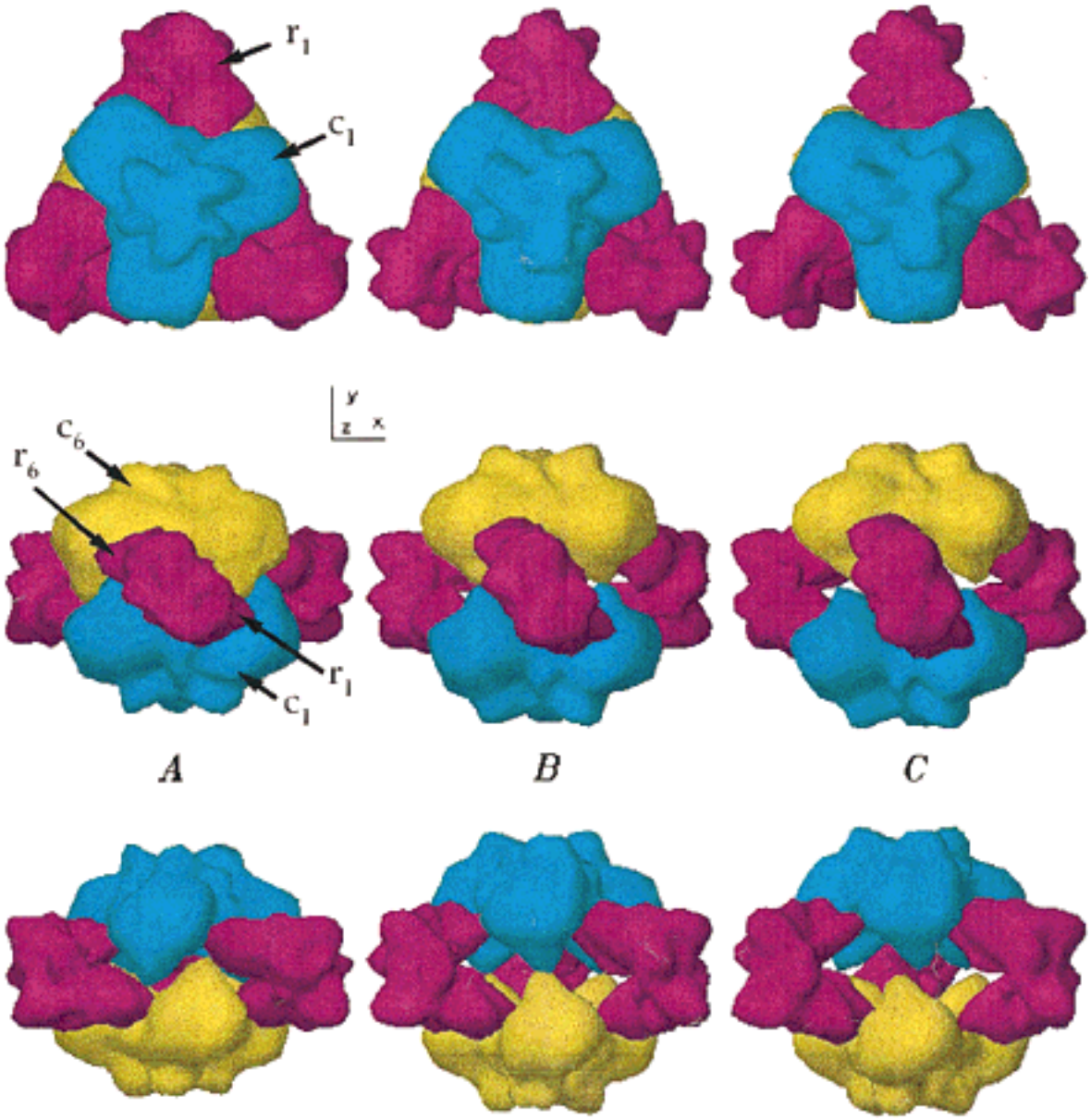

Fig. 1. Models of ATCase quaternary structure "as seen" by x-rays at low resolution (see Materials and Methods). The two c trimers are colored in yellow and cyan, the three r dimers in magenta. **Top:** View along the threefold axis (Z) from the side of the lower c trimer c_1—c_3. **Middle** and **bottom:** Views along one of the twofold axes (top view rotated along *x* axis by 90° counterclockwise and clockwise, respectively). In each row, A and B are the crystal structures of the T and R states, respectively; C is the model of the R-state in solution. The domains are represented by the envelope functions as evaluated by the program CRYSOL. Axial unit, 2 nm.

the present paper we use a method[16] that takes solvent effects into account to prove that the movements of the subunits during the T → R transition in solution are significantly larger than those in the crystals.

MATERIALS AND METHODS

Sample Preparation and Scattering Experiments

X-ray scattering patterns were recorded on the D24 small-angle scattering instrument, installed on a bending magnet of the storage ring LURE-DCI (Orsay, France) using a wavelength λ = 0.149 nm and sample to detector distances of 1.2 and 2 m with linear and quadrant position-sensitive detectors. All enzyme solutions were prepared in 50 mM Tris HCl pH 8.3, 1 mM dithiotreitol and examined at room temperature. T-state solutions contained unligated enzyme; for the R state a twofold molar excess of the transition state analogue PALA (*N*-phosphonacetyl-L-aspartate) was added.[17] A concentrated solution of

ATCase was loaded onto a gel filtration HPLC column to elinate the small amount of dimers occasionally observed, the top of the monomer peak was collected and its concentration adjusted immediately before x-ray measurements. The resulting curves yielded linear Guinier plots[18] without any indication of higher molecular weight contaminant, as confirmed by HPLC. Eight successive frames of 100 seconds each were recorded for each sample. Each frame was visually checked for radiation damage—none was found—before computing the average and the standard deviation of the data. Background-corrected curves measured with 4, 20, and 50 mg ATCase/ml were scaled and spliced to cover the range of the scattering vector $0.09 < s < 3.2$ nm^{-1} ($s = (4\pi/\lambda) \sin\theta$, where 2θ is the scattering angle). Data sets recorded with different enzyme preparations and detectors over several years coincide within the present error bars. Scattering curves of both T-state and R-state solutions were also recorded in 50 mM imidazole buffer pH 7.0, 1 mM dithiotreitol. They are identical to those obtained at pH 8.3.

Theory and Data Analysis

The scattering intensity $I(s)$ from particles in a solvent with scattering length density ρ_0 can be evaluated as

$$I(s) = <|A_a(\mathbf{s}) - \rho_0 A_c(\mathbf{s}) + A_b(\mathbf{s})|^2>_\Omega \qquad (1)$$

where $A_a(\mathbf{s})$, $A_c(\mathbf{s})$ and $A_b(\mathbf{s})$ are the amplitudes from the particle in vacuo, the excluded volume, and the hydration shell, respectively. Here $< \ldots >_\Omega$ stands for the average over all particle orientations and Ω is the solid angle in reciprocal space, $\mathbf{s} = (s,\Omega)$.

The coordinates of ATCase were taken from the Brookhaven Protein Data Bank, entries 6at1 (T state)[5] and 8atc (R state).[11] Each file contains the asymmetric unit involving a lower (r_1c_1) and an upper (r_6c_6) rc unit related by a noncrystallographic twofold axis. Those were triplicated using the threefold axis to yield the holoenzyme.

Scattering intensities were evaluated from the crystal structures using the program CRYSOL.[16] The particle shape is approximated by an angular envelope function, and the scattering intensities in Equation (1) are expressed in terms of spherical harmonics to speed up the calculations. The scattering from the hydration shell is simulated by surrounding the envelope function with a layer of thickness $\Delta = 0.3$ nm and density ρ_b. The experimental scattering curves $I_o(s_i)$ are fitted using two parameters, the total excluded volume, V, and the contrast of the border layer $\delta\rho = \rho_b - \rho_o$, to minimize the discrepancy χ defined as

$$\chi^2 = \frac{1}{N-1} \sum_{i=1}^{N} \left(\frac{I_e(s_i) - I(s_i)}{\sigma(s_i)} \right)^2 \qquad (2)$$

where N is the number of experimental points and $\sigma(s_i)$ are the standard deviations.

Solid body illustrations in Figure 1 were produced on a SPARC-20ZX Sun workstation with the program ASSA (M. B. Kozin and D. I. Svergun, unpublished), which uses spherical harmonics to describe the protein envelope, that is, the very description used to calculate the scattering patterns. Figure 1 is thus a faithful representation of the enzyme as "seen" by the x-rays at the low resolution of our experiments. Atomic structures were displayed on a Silicon Graphics Indigo^2 workstation using the program "O".[19]

RESULTS

The best agreement (discrepancy $\chi = 2.6$) between the theoretical and experimental profiles for the T state (Figure 2) is obtained for $V = 401$ nm^3 and $\delta\rho = 68$ e/nm^3, corresponding to a hydration of 0.23 (w/w). If the hydration shell is not taken into account, the best fit is much poorer ($\chi = 8.8$) and the observed deviations (dashed-dotted curve in Fig. 2) correspond to those reported by Altman and colleagues.[15] The quaternary structures of the T state in solution and in the crystal should thus not differ and the discrepancies[15] are indeed due to the neglect of solvent effects. The radii of gyration calculated from the experimental curve ($R_g = 4.67 \pm 0.03$ nm) and the T crystal structure with ($R_g = 4.64$ nm) and without ($R_g = 4.40$ nm) hydration shell illustrate the magnitude of the latter's contribution. Minor differences in intensity of the high-angle maxima for the best fit (in the momentum transfer range $s > 2$ nm^{-1}), are most probably due to differences in the tertiary structure.

Although accounting for the hydration shell improves the fit for the R state—the χ value drops from 8.2 to 4.8, and the R_g increases from 4.62 to 4.81 nm—the best fit to the experimental data giving $V = 397$ nm^3 and $\delta\rho = 90$ e/nm^3 remains poor (Fig. 2). Systematic deviations near the origin of the scattering curve (the experimental $R_g = 4.95 \pm 0.03$ nm) and around the first subsidiary maximum (the range of momentum transfer $0.5 < s < 1$ nm^{-1} corresponding to a resolution of 5–10 nm) point to a significant difference between the quaternary structures of the R state in the crystal and in solution.

A comparison of the curves in Figure 2 indicates that in the vicinity of the first subsidiary maximum the scattering curve from the crystal structure of the R state lies between those of the T state and the experimental data of the R state. This suggests that the model of the R state in solution may be obtained by moving the crystal structure farther away from the T state along the path of the T → R transition found in the crystals.

For this purpose and in keeping with the low resolution of solution x-ray scattering patterns we restricted the modeling to rigid body movements

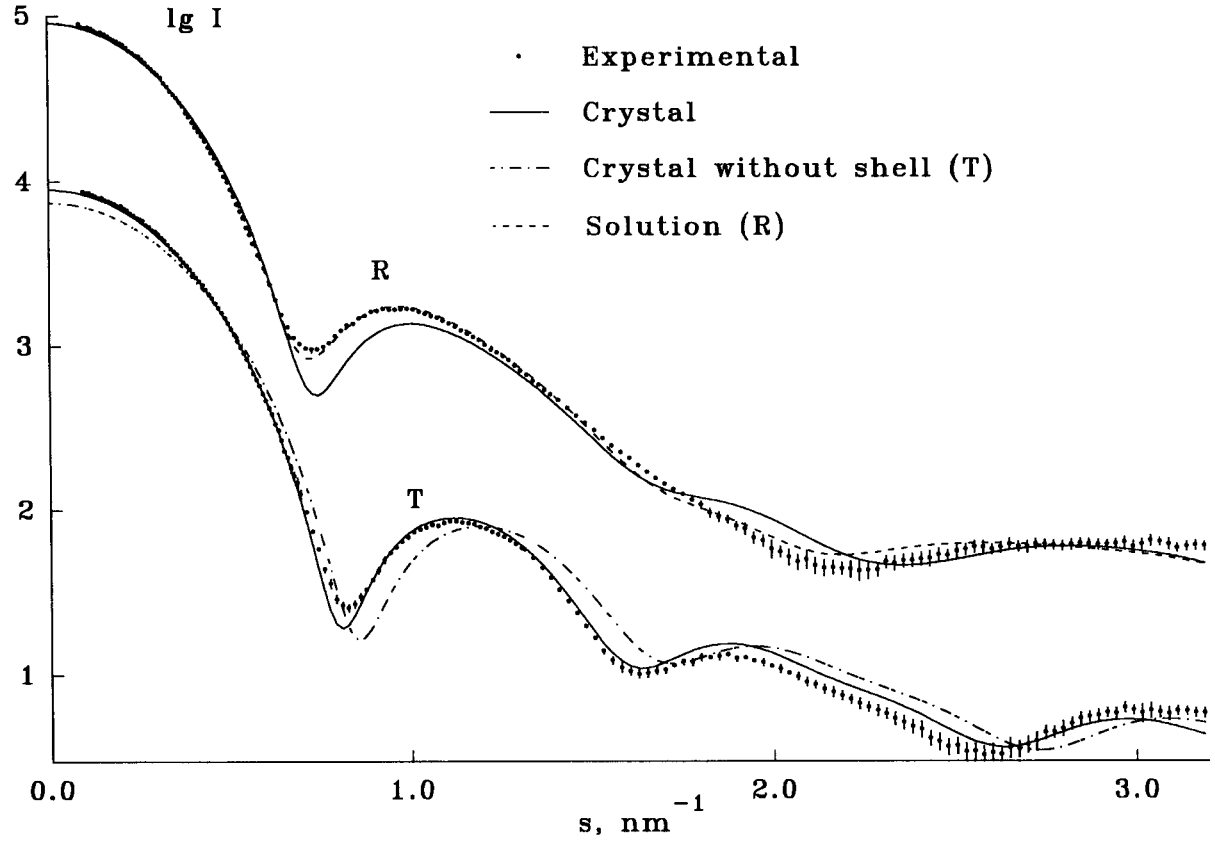

Fig. 2. Comparison of the solution scattering data of ATCase with the scattering from the atomic structures for the T and R states. The curves from R state were shifted by one logarithmic unit for better visualization. The evaluated curves for the T-state correspond to the model in Figure 1A, those for the R state to the models in Figure 1B and C. Error bars correspond to $\pm\sigma$.

following the description of the T → R transition mentioned in the introduction.[10–12] This involves translations and rotations obeying D_3 symmetry of the two c trimers of the crystal structure of the R state along the threefold axis, and the three r dimers along the corresponding twofold axes. In order to preserve the contacts between r_1 and c_1 chains, coordinates of the center of the r_1-c_1 interface, which is barely affected in the T → R transition[11], were determined, after discarding a few contacts at the edges of the interface. Displacements of this point correlate the translations and rotations of the two chains so that the whole operation is defined by a single parameter (e.g., the distance between the c trimers). The best fit was calculated for a set of structures corresponding to different displacements (the excluded volume *V* of the models varied by less than 1.5%).

Figure 3 presents the discrepancy between the experimental scattering from the R-state and that of the models versus the increase of the distance Δd between the c trimers ($\Delta d = 0$ is the R crystal structure). The plot displays a clear minimum at $\chi = 1.8$ for $\Delta d = 0.34$ nm. Taking the R crystal structure as reference, this implies the rotation of the c trimers by 11° in opposite directions around the threefold axis. Simultaneously, each of the three r dimers is rotated by 9° around the corresponding twofold axis and displaced by 0.14 nm away from the molecular center along this axis (Fig. 1C). The fit to the experimental data (dashed line in Fig. 2) corresponds to $V = 402$ nm^3 and $\delta\rho = 70$ e/nm^3, that is, practically the same parameters as for the T-structure. The radius of gyration of the final model $R_g = 4.96$ nm neatly fits the experimental value.

The differences between the R state crystal structure and the solution model are thus anything but marginal. The root mean square deviation (rms) of the Cα-coordinates in the crystal structures of the T and R states is 0.62 nm. That between our model and either T state (rms = 0.99 nm) or R state (rms = 0.46 nm) crystal structures indicate that the overall changes accompanying the T → R transition in solution are about 50% larger than in the crystal. In terms of the individual domains, the increase in the separation between the two c trimers is 30% larger in solution than in the crystal, while the accompanying rotations around the threefold and twofold axes represent, respectively, about twice and half that observed in the crystal after the T to R transition.

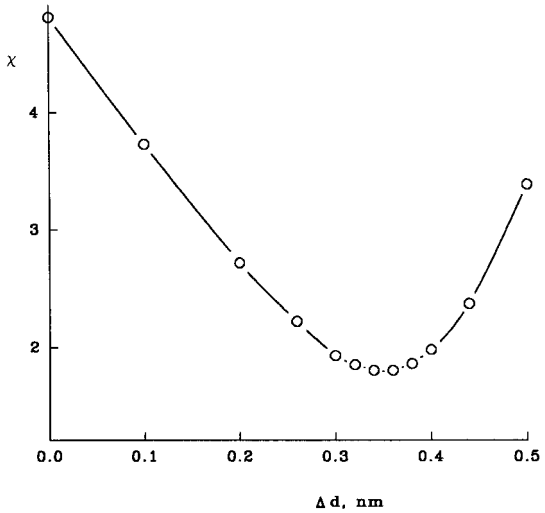

Fig. 3. Discrepancy χ between the experimental data and the scattering from the model of the R state as a function of the increase in distance between the c-trimers coupled with the movements of subunits as described in the text. $\Delta d = 0$ corresponds to the R crystal structure and $\Delta d = 0.34$ nm to the final model in solution.

DISCUSSION

Solution scattering provides low-resolution structural information and its interpretation in terms of high-resolution structures requires caution. The observed agreement for the T state thus only constitutes a strong argument in favor of the identity of the crystal and solution structures, not an unequivocal proof. For the R state, the significant disagreement with the solution scattering data by no means invalidates the crystal structure as such but does prove the difference in the quaternary structures between the crystal and solution forms.

Could the differences between the solution and the crystal structures be ascribed to the differences in the physicochemical conditions under which both studies have been conducted? Crystals were first grown at pH 5.8, close to the isoelectric point of the protein.[10,13,20] Scattering patterns collected on pellets of ATCase with and without PALA at pH 6.0 are in qualitative agreement with the changes observed in solution, suggesting that a similar change in quaternary structure occurs at low pH, though the data would not allow to distinguish between the two R structures (Vachette et al., unpublished results). Subsequently crystallizations were performed at pH 7.0, and the T and R crystal structures recorded at neutral pH were shown to be very similar to the structures obtained at pH 5.8.[21] Scattering patterns of unligated and PALA-bound enzyme solutions at pH 7.0 (though without precipitating agent) are identical to those obtained at pH 8.3. Neither the crystal structure nor the solution structures appear to be significantly altered by pH. The ideal test, which would consist in recording scattering patterns on solutions of enzyme under crystallization conditions, cannot be made in practice, especially if one considers the high concentration of enzyme required.

Taking proper account of the scattering contribution from hydration water is a central question in the calculations of scattering patterns from crystallographic coordinates. In vacuo calculations as performed by Altman et al.[15] lead to the systematic deviations also observed here in the absence of hydration shell (Fig. 2). Addition of the hydration layer leads to an agreement with the experimental data for the T state but not for the R state. Generating the hydration layer only around the outer molecular envelope somewhat underestimates the scattering contribution from the shell of bound water lining the central cavity of the enzyme. This, however, has only a marginal effect on the resulting scattering pattern, as this shell represents at most 5% of the total bound water [note that the bulk water outside the hydration layer but in the central cavity which has a scattering length density ρ_0 is taken into account in Eq. (1)]. To rule out the possibility that the increase in size of the cavity in the R-state would explain the discrepancy between the calculated and the experimental scattering patterns, control calculations were made with the models of the R state divided into lower and upper parts for which the complete hydration shells including those of the walls of the central cavity were evaluated separately. This overestimates the effect since the r–r interfaces are not hydrated in the complete enzyme. For the crystal R state ($\Delta d = 0$) χ increases to 5.3 and drops to 1.9 at $\Delta d = 0.4$ nm. The main conclusions remain unchanged with a slightly increased Δd value (0.4 nm instead of 0.34 nm).

Some tertiary changes have been shown to play an important role in the transition between the two crystal structures, among which an average opening of about 9° of the interface between the two domains of the regulatory chain.[6] The elongation observed in solution might thus well be accompanied by an increase in this opening. Such a likely movement involving well defined but small domains would produce only minor changes in the scattering profile. In keeping with the low resolution of our experimental data, no attempt was made to model possible changes in tertiary structure and the interpretation was restricted to rigid body movements of the subunits.

As already mentioned, the three twofold axes are non-crystallographic and the crystal structures of T and R states both have only quasi-D_3 symmetry. Analysis shows that the deviations from the noncrystallographic symmetry in the T structure are, however, local and correspond to individual residues,

whereas the larger discrepancies in the R state affect entire domains as pointed out earlier.[20] This strongly suggests that the R state crystal structure may be distorted compared to the isotropic environment in solution. The model in Figure 1C was obtained without averaging the noncrystallographic symmetry related subunits. Imposing D_3 symmetry by averaging the quasi-equivalent r–c units (e.g., r_1c_1 and r_6c_6) yields practically identical results. Generating the D_3-symmetric models starting from either r_1c_1 or r_6c_6 worsens the fit ($\chi = 2.6$ for $\Delta d = 0.38$ nm and 2.1 for $\Delta d = 0.30$ nm). This modeling provides an estimate of the uncertainty of the Δd value while suggesting that the structure of the r–c unit in solution is likely to be in between that of the r_1–c_1 and r_6–c_6 units.

In the model of the R state in solution, the c trimers reach practically an eclipsed position. Their larger separation causes the rupture of their common interface located at the 240s loops in the crystal structure, as clearly seen on the last row of Figure 1. Preservation of the contacts between the 240s loops would require them to adopt a more extended conformation but this change is most likely opposed by the links between Glu239 and both Lys164 and Tyr165. In contrast, the interface between the c_i and r_i chains seems to be reinforced by the tighter packing of these chains in the solution model compared to the crystal structure (Fig. 4). The region around residue 130 in the r chain continues its movement towards the equatorial domain of the c chain around residue 200 thereby creating more opportunities for interchain contacts. Since the tertiary structure was not modified, our model displays minor overlaps of the two chains which mainly involve side chains and can be corrected by rotating them. Only one Cβ atom in the regulatory chain is closer than 0.27 nm to the backbone of the catalytic chain.

The crystal structure of the R-state has been studied using different combinations of substrate analogues—PALA,[11,20] carbamyl phosphate and succinate[22] as well as phosphonoacetamide and malonate[21]—and different crystallization conditions. Although the PALA-aspartate transcarbamylase complex has been crystallized in three different space groups,[10] all the published structures just mentioned have been determined in crystals of space group P321, that is, under the same packing constraints. All structures are identical and only differ in some details at the active site. This supports the validity of the crystal structure determinations, which is not in any way questioned by our work. The identity of the quaternary structures of the R state is also observed in solution where the scattering patterns of ATCase saturated with PALA or with carbamyl phosphate and succinate are practically undistinguishable. At that point, it is tempting to speculate

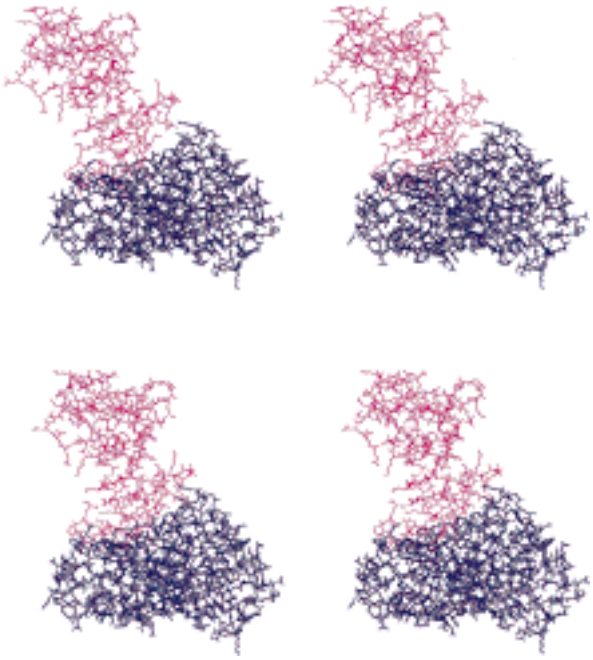

Fig. 4. Stereo view along the threefold axis of the c_1-(blue) and r_1-(magenta) subunits in the R state for the crystal structure in Figure 1B (top) and the solution model in Figure 1C (bottom).

that the crystal structure of the R state represents a transient intermediate along the transition path between T and R. The likely explanation for its existence within the crystal is best formulated by Krause et al.[20]: "The stacking of the 240s loops on top of each other . . . prevents a reversion to the T form via a simple collapse along the 3-fold axis."

We may ask ourselves whether the quaternary structure observed in the crystal may be present in significant amounts in solution. We have only one piece of evidence provided by SAXS measurements. Titration experiments performed using variable concentrations of PALA could detect the presence in solution of only two quaternary structures[17] and similar observations have been made in the presence of carbamyl phosphate and succinate.[23] Accordingly, no significant amount of molecules in the R-state crystal conformation, which would have been detected in our titration experiments by requiring a third quaternary structure, can be found in solution.

Two R structures have already been reported for haemoglobin, the other paradigm of allosteric proteins.[24] Following the crystal structure determination and refinement of oxy (R) and deoxy (T) hemoglobin,[24,25] a third quaternary structure was characterized in a carbonmonoxy mutant hemoglobin called Ypsilanti.[26] A geometrical analysis of the allosteric Y state quaternary structure by Janin and Wodak[27] indicated that Y is a modified R state rather than an intermediate on the T to R pathway. A similar to Y

quaternary structure denoted R2 was then observed on crystals of liganded hemoglobin grown in "low salt" conditions.[28] The authors proposed that the R2 state may function as a stable intermediate along a R–R2–T pathway. A reexamination of the relationship between the three quaternary forms led Srinivasan and Rose[29] to the suggestion that R may lie on the pathway from T to R2. The authors tentatively concluded that, under physiological conditions, only two distinct populations, T and R2, coexist in solution. While two crystal structures of the R-state are compared in the case of hemoglobin, and conclusions are extrapolated to the situation in solution, in the case of ATCase we deal with two structures of the R state, one in the crystal, the second one in solution.

Ligand binding and conformational changes in allosteric enzymes involve only low-energy noncovalent interactions. The activation energy of the quaternary structure transition is thus also low and the crystal packing forces originating from noncovalent bonds between neighboring molecules may distort the architecture of proteins selected for easy reorganization.

The present study clearly illustrates that it is essential, especially in the case of multidomain macromolecules, to test crystal structures against solution scattering data. Integration of this complementary information into computer models provides a tool for analyzing differences (if any) in terms of plausible changes in the quaternary structure while stimulating in parallel renewed crystallographic attempts.

ACKNOWLEDGMENTS

We thank M. Kozin for help in computer graphics, P. Tauc, M. Renouard, and M. Garrigos for help with the enzyme purification and W. N. Lipscomb for his insightful suggestions about the manuscript. This work was supported by NATO Linkage grant LG 921231, INTAS grant 93–645, LIP Contract CHGE-CT93–0040 of the European Union, and the CNPq fellowship from the Conselho Nacional de Desenvolvimento Científico e Tecnológico (Brasil) to C. Barberato. P. V. acknowledges support by the CNRS.

REFERENCES

1. Stryer, L. "Biochemistry." New York: W.H. Freeman, 1995.
2. Reichard, P., Hanshoff, G. Aspartate carbamyl transferase from *Escherichia coli*. Acta Chim. Scand. 10:548–566, 1956.
3. Yates, R.A., Pardee, A.B. Control of pyrimidine biosynthesis in *Escherichia coli* by a feed-back mechanism. J. Biol. Chem. 221:757–770, 1956.
4. Kantrowitz, E.R., Lipscomb, W.N. *Escherichia coli* aspartate transcarbamylase: The relation between structure and function. Science 241:669–674, 1988.
5. Stevens, R.C., Gouaux, J.E., Lipscomb, W.N. Structural consequences of effector binding to the T state of aspartate carbamoytransferase: Crystal structures of the unligated and ATP and CTP-complexed enzymes at 2.6 A resolution. Biochemistry 29:7691–7701, 1990.
6. Lipscomb, W.N. Aspartate transcarbamoylase from Escherichia coli: activity and regulation. Adv. Enzymol. 68:67–151, 1994.
7. Monod, J., Wyman, J., Changeux, J.P. On the nature of allosteric transitions. A plausible model. J. Mol. Biol. 12:88–118, 1965.
8. Gerhart, J.C., Schachman, H.K. Allosteric interactions in aspartate transcarbamylase. II. Evidence for different conformational states of the protein in the presence and absence of specific ligands. Biochemistry 7:538–552, 1968.
9. Howlett, G.J., Schachmann, H.K. Allosteric regulation of aspartate transcarbamoylase: Changes in the sedimentation coefficient promoted by the bisubstrate analogue *N*-(phosphonacetyl)-L-aspartate. Biochemistry 16:5077–5083, 1977.
10. Ladner, J.E., Kitchell, J.P., Honzatko, R.B., Ke, H.M., Volz, K.W., Kalb (Gilboa), A.J., Ladner, R.C., Lipscomb, W.N. Gross quaternary changes in aspartate carbamoyltransferase are induced by the binding of *N*-(phosphonacetyl)-L-aspartate: A 3.5-A resolution study. Proc. Natl. Acad. Sci. USA 79:3125–3128, 1982.
11. Ke, H.-M., Lipscomb, W.N., Cho, Y., Honzatko, R.B. Complex of *N*-phosphonacetyl-L-aspartate with aspartate transcarbamoylase: X-ray refinement, analysis of conformational changes and catalytic and allosteric mechanisms. J. Mol. Biol. 204:725–747, 1988.
12. Stevens, R.C., Chook, Y.M., Cho, C.Y., Lipscomb, W.N., Kantrowitz, E.R. *Escherichia coli* aspartate carbamoyltransferase: the probing of crystal structure analysis via site-specific mutagenesis. Protein Eng. 4:391–408, 1991.
13. Monaco, H.L., Crawford, J.L., Lipscomb, W.N. Three-dimensional structures of aspartate carbamoyltransferase from *Escherichia coli* and of its complex with cytidine triphosphate. Proc. Natl. Acad. Sci. USA 75:5276–5280, 1978.
14. Moody, M.F., Vachette, P., Foote, A.M. Changes in the X-ray solution scattering of aspartate transcarbamoylase following the allosteric transition. J. Mol. Biol. 133:517–532, 1979.
15. Altman, R.B., Ladner, J.E., Lipscomb, W.N. Quaternary structural changes in aspartate carbamoyl transferase EC 2.1.3.2 of *Escherichia coli* at pH 8.3 and pH 5.8. Biochem Biophys. Res. Commun. 108:592–595, 1982.
16. Svergun, D.I., Barberato, C., Koch, M.H.J. CRYSOL: A program to evaluate x-ray solution scattering of biological macromolecules from atomic coordinates. J. Appl. Crystallogr. 28:768–773, 1995.
17. Fetler, L., Tauc, P., Herve, G., Moody, M.F., Vachette, P. X-ray scattering titration of quaternary structure transition of aspartate transcarbamylase with a bisubstrate analogue: Influence of nucleotide effectors. J. Mol. Biol. 251:243–255, 1995.
18. Guinier, A., Fournet, G. "Small-Angle Scattering of X-rays." New-York: Wiley, 1955.
19. Jones, T.A., Zou, J.-Y., Cowan, S.W., Kjeldgaard, M. Improved methods for building protein models in electron density maps and the location of errors in these models. Acta Crystallogr. A47:110–119, 1991.
20. Krause, K.L., Volz, K.W., Lipscomb, W.N. 2.5 A structure of aspartate carbamoyltransferase complexed with the bisubstrate analog *N*-(phosphonacetyl)-L-aspartate. J. Mol. Biol. 193:527–553, 1987.
21. Gouaux, J.E., Lipscomb, W.N. Crystal structures of phosphonoacetamide ligated T and phosphonoacetamide and malonate ligated R states of aspartate carbamoyltransferase at 2.8-A resolution and neutral pH. Biochemistry 29:389–402, 1990.
22. Gouaux, J.E., Lipscomb, W.N. Three-dimensional structure of carbamoyl phosphate and succinate bound to aspar-

tate carbamoyltransferase. Proc. Natl. Acad. Sci. USA 85:4205–4208, 1988.
23. Tsuruta, H., Vachette, P., Sano, T., Moody, M.F., Amemiya, Y., Wakabayashi, K., Kihara, H. Kinetics of the quaternary structure change of aspartate transcarbamylase triggered by succinate, a competitive inhibitor. Biochemistry 33: 10007–10012, 1994.
24. Fermi, G., Perutz, M.F., Shaanan, B., Fourme, R. The crystal structure of human deoxyhaemoglobin at 1.74 Å resolution. J. Mol. Biol. 175:159–174, 1984.
25. Shaanan, B. Structure of human oxyhaemoglobin at 2.1Å resolution. J. Mol. Biol. 171:31–59, 1983.
26. Smith, F.R., Lattman, E.E., Carter, C.W., Jr. The mutation b99 Asp-Tyr stabilizes Y: A new, composite quaternary state of human hemoglobin. Proteins 10:81–91, 1991.
27. Janin, J., Wodak, S.J. The quaternary structure of carbonmonoxy hemoglobin Ypsilanti. Proteins 15:1–4, 1993.
28. Silva, M.M., Rogers, P.H., Arnone, A. A third quaternary structure of human hemoglobin A at 1.7Å resolution. J. Biol. Chem. 267:17248–17256, 1992.
29. Srinivasan, R., Rose, G.D. The T-to-R transformation in hemoglobin: A reevaluation. Proc. Natl. Acad. Sci. USA 91:11113–11117, 1994.